Jour.Korean Inst.Mining Geol.
Vol.24, No.3, p.233-244,1991.

Supergene Chloritization and Vermiculitization in Hornblende Gneiss, the Cheongyang Area, Korea

Yungoo Song* and Hi-Soo Moon*

ABSTRACT: A biotite that substantially altered to chlorite and vermiculite in hornblende gneiss from Cheonyang, Korea, has been investigated with electron microprobe analysis. The data show the general variational trends of Ti and K-leaching with increased weathering. However, the chloritization is characterized by Si- conservative reaction and relatively dramatic increase of Al-for-(Fe+Mg) octahedral substitution, whereas the vermiculitization is characterized by total Mg-conservative and Ca-enriching exchange reaction. In the initiating stage the vermiculitization proceeded in a continuous decrease of the Al-for-Si tetrahedral substitution and an increase of the Al-for-(Fe+Mg) octahedral substitution, supporting the currently accepted weathering process. But it differs in the late stage, in which Al(Ⅳ) and Fe increase significantly. Recalculations of the structural formular for vermiculite on the basis of several assumptions indicate that the oxidation of Fe is necessary for vermiculite to form the reasonable strutural formular. The relative timing of the oxidation of Fe probably occurs in the late stage, supported by the substantial increase of the Al-for-Si tetrahedral substitution.

INTRODUCTION

Solid-state transformations of one sheet silicate into another occur commonly in nature. Chloritization and vermiculitization of trioctahedral micas inherited from basic igneous rock under earth-surface conditions are important examples. Recent studies of the alteration of rock-forming phyllosilicates by supergene alteration processes suggest the detailed reaction mechanisms involved in the replacement processes by using the high resolution transmitted electron microscope (HRTEM) and analytical TEM methods (Ferry, 1979 ; Iijima and Zhu, 1982 ; Veblen, 1983 ; Veblen and Ferry, 1983 ; Olives and Amouric, 1984 ; Yau et al .,1984 ; Eggleton and Banfield, 1985 ; Banfield and Eggleton, 19880).

Ferry(1979) found that in an assumed Al-conservative alteration of granitic biotite to chlorite there was a 18.6% volume decrease, and that Mg^{2+} and Fe^{2+} ions are added. Veblen and Ferry (1983) proposed two possible chloritization mechanisms and showed that the chloritization proceeded by the replacement of TOT (tetrahedron-octahedron-tetrahedron) layers in biotite by brucite-like layers was dominant mechanism, with consequential volume loss of 30%. On the other hand,Olives and Amouric(1984) concluded that the chloritization occurs by brucitization of the potassium plane, in the contrast to Veblen and Ferry's dominant mechanism. And Yau et al.(1984) observed the volume-preserving transformation of 14 phlogopite layers terminating against 10 chlorite layers which indicates that pervasive replacement may occur through a combination of both reactions. The transformation process of biotite to vermiculite has also received considerable attention from many mineralogists. Those two mechanisms were also showed in the transformation processes of biotite to vermiculite by TEM observations (Banfield and Eggleton, 1988). The biotite in hornblende gneiss, distributed in the Cheongyang area, Korea, is characterized by the recognition of both alteration processes. In the present study, the authors describe the detailed chemical variations in the chloritization and vermiculitization undergone by the biotite from hornblende gneiss in Cheongyang, Korea, based on the two transformation mechanisms mentioned above and the systematic microprobe analyses data and also discuss the difference between the chloritization and vermiculitization of the biotote in the aspect of elements gain-and-loss relations, especially.

* Department of Geology, Yonsei University, Seoul 120-749, Korea

SAMPLE DESCRIPTION AND ANALYTICAL METHODS

The sample employed in this study is from the hornblende gneiss in Cheongyang, Korea (Fig. 1). The hornblende gneiss, which intruded the Precambrian metasediments, is originated from age-unknown mafic magmatism and affected by several metamorphisms. It mainly consists of hornblende, biotite, plagioclase, alkali feldspar, and a small amount of garnet, clinopyroxene, quartz, and opaque minerals. The biotite has altered partially on a scale easily observable in thin section to chlorite in relatively less altered samples and to vermiculite in more altered samples. Sphene and epidote are also observed less commonly as weathering products in some samples. Samples were collected randomly from several outcrops and these localities are presented in Fig.1. For the purpose of this study, the polished thin sections of the selected samples were prepared for the conventional petrographic and subsequent electron microprobe examinations. Chemical analyses for several minerals in the gneiss were performed with a JEOL JCXA-733 model electron microprobe analysis ; wave-dispersive detector was used with a standard Bence and Albee (1968) correction procedure, a beam current of 1.5×10^{-8} A, beam diameter of 10 μm and a counting time of 80 sec. Natural silicates and oxide minerals were used for the standard materials. Alkali elements were measured first of all in measurment sequences.

ANALYTICAL RESULTS

Chemical data derived by microprobe analysis for several minerals of the representative samples were listed in Table 1. The ferrous Fe contents in amphiboles were recalculated on the basis of the stoichiometry by Spear and Kimball (1984) method and total Fe contents in other minerals were assumed to be in the ferrous state.

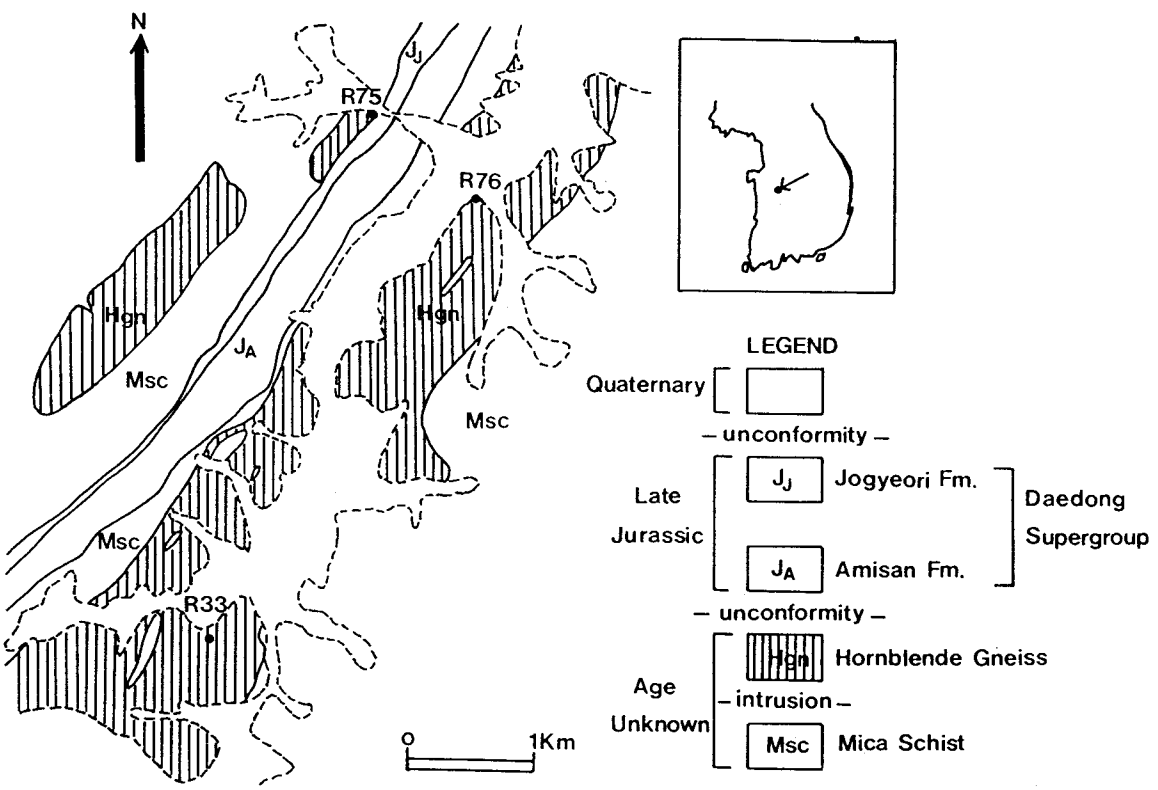

Fig. 1. Simplified geological map and sample localities of the Cheongyang area, Korea.

The amphibole is a common hornblede and reveals the substitution of Al(Ⅳ) (Al in tetrahedral site), K, and Na for Si for the charge balance. The trioctahedral mica is a titaniferous biotite and characterized by being essentially free of Al (VI)(Al in octahedral site) (about 0.3 atomic %) and the wide range of the Fe contents (FeO ≒ 15~24 wt.%). The chlorite is a ripidolite to pycnochlorite and the vermiculite is characterized by relatively high Ca contents (CaO ≒ 0.7~1.3 wt.%) compared with the biotite and chlorite. The sphene and garnet, Ca-rich phases, are the alteration and metamorphic products, respectively, and the garnet has typically high grossular component (Xgrossular≒ 0.38).

Representative microprobe analyses of the biotite and their chloritized (R75, R76) and vermiculitized (R33) products are also presented in Table 2 and 3, respectively. All Fe contents were assumed to be in ferrous state and octahedral

Table 1. Electron microprobe analyses and structural formulae for representative minerals.

Element	Hornblende		Biotite	Chlorite		Vermiculite	Sphene	Garnet
	R75	R76	R75	R75	R76	R33	R75	R75
SiO_2	42.45	40.51	35.32	26.16	27.08	30.56	30.83	38.98
TiO_2	0.77	2.20	2.85	0.12	0.07	0.10	36.38	0.11
Al_2O_3	14.38	12.44	15.31	18.74	20.38	18.59	1.92	21.88
Fe_2O_3	1.94	2.09	0.00	0.00	0.00	0.00	0.00	0.00
FeO	15.89	14.74	24.66	29.32	20.08	24.94	0.29	23.24
MnO	0.25	0.31	0.23	0.33	0.39	0.18	0.00	0.82
MgO	8.73	10.07	8.77	12.58	19.02	9.43	0.01	2.44
CaO	11.49	11.34	0.13	0.00	0.00	0.63	28.38	13.69
Na_2O	1.39	1.89	0.06	0.02	0.01	0.10	0.00	0.01
K_2O	1.62	1.73	8.27	0.02	0.03	0.64	0.01	0.00
Total	98.91	97.32	95.60	87.29	87.06	85.17	97.82	101.17
	O(23)		O(22)	O(28)		O(22)	O(10)	O(24)
Si	6.304	6.155	Si 5.497	Si	5.669	5.583	Si 5.157	Si 2.049	6.026
Al(IV)	1.696	1.845	Al(IV) 2.503	Al(IV)	2.331	2.417	Al(IV) 2.843	Al 0.150	3.986
								Ti 1.819	0.013
Al(VI)	0.821	0.383	Al(VI) 0.305	Al(VI)	2.455	2.536	Al(VI) 0.853	Fe* 0.016	3.004
Ti	0.086	0.251	Ti 0.334	Ti	0.020	0.011	Ti 0.013	Mn 0.000	0.107
Fe^{3+}	0.217	0.239	Fe* 3.210	Fe*	5.313	3.462	Fe* 3.519	Mg 0.001	0.562
Fe^{2+}	1.973	1.873	Mn 0.030	Mn	0.061	0.068	Mn 0.026	Ca 2.021	2.267
Mn	0.031	0.040	Mg 2.035	Mg	4.064	5.846	Mg 1.589	Na 0.000	0.003
Mg	1.933	2.281	5.914	Ca	0.000	0.000	6.000	K 0.001	0.000
	5.061	5.068		Na	0.008	0.004			
			Ca 0.022	K	0.006	0.008	Mg 0.783		
XM1-3	0.061	0.068	Na 0.018		11.926	11.935	Ca 0.114		
Ca	1.828	1.846	K 1.642				Na 0.033		
Na(M4)	0.110	0.086	1.682				K 0.138		
							1.067		
Na(A)	0.290	0.471							
K	0.307	0.335							
	0.597	0.806							

*Total Fe assumed to be in ferrous.

sites of vermiculitized products to be in complete occupancy. Structural formulae for the altered biotite to chlorite were recalculated on the basis of 25 oxygens. Altered biotites reveal the intermediate in chemical compositions. TEM observations (Veblen,1983 ; Veblen and Ferry, 1983 ; Olives and Amouric, 1984 ;Yau et al.,1984 ; Banfield and Eggleton, 1988) indicate that biotite transformed through the interstratifications of biotite/chlorite and biotite/vermiculite to chlorite and vermiculite in general. Otherwise the altered biotites can be considered as interstratifications of biotite/chlorite and biotite/vermiculite. Microprobe beam diameter is 10㎛ which means that the microprobe data indicate the composite chemical compositions of a numerous number of biotite and chlorite or vermiculite layers, and the increase of alterations indicates the increase of the percentage of the chlorite or vermiculite layers.

These data show apparently the common variational trends of Si, Ti and K-leaching and Al, Fe-enriching in both alteration processes. However, distinct enrichment of the Mg contents as weathering increases is general trend in the chloritization, whereas the vermiculitization, which is characterized by Ca-enriching does not show this trend and has relatively narrow variational extent of constituents. Entrance of a substantial number of the Ca contents in the vermiculitization that is one of the distinct differences between two alteration processes can be considered as the interlayer cation inherited from alteration reactions of Ca-enriched phases in hornblende gneiss. Substitutional relations between Si, Al, Fe, and Mg in mica-like layer for the

Table 2. Electron microprobe analyses and structural formulae for biotites and altered products to chlorites.

Element	R75					R76					
	1	2	3	4	5	1	2	3	4	5	6
SiO_2	35.32	34.52	26.67	26.46	25.99	34.41	31.53	31.77	28.66	27.45	27.08
TiO_2	2.85	2.26	0.06	0.13	0.06	1.92	3.45	1.08	0.08	0.06	0.07
Al_2O_3	15.31	15.63	18.84	19.55	19.98	16.34	16.54	17.83	19.03	20.05	20.38
FeO*	24.66	24.82	29.62	29.40	28.40	19.12	17.84	19.22	20.45	19.93	20.08
MnO	0.23	0.22	0.30	0.37	0.38	0.32	0.29	0.30	0.38	0.37	0.39
MgO	8.77	9.38	12.83	12.74	12.58	14.12	14.78	16.24	18.31	18.61	19.02
CaO	0.13	0.00	0.01	0.00	0.00	0.04	0.99	0.03	0.04	0.03	0.00
Na_2O	0.06	0.06	0.00	0.04	0.02	0.08	0.04	0.03	0.01	0.00	0.01
K_2O	8.27	7.43	0.03	0.02	0.03	6.83	4.82	3.96	0.75	0.04	0.03
Total	95.60	94.32	88.36	88.71	87.44	93.18	90.28	90.46	87.71	86.54	87.06
	O(22)		O(28)			O(25)			O(28)		
Si	5.497	5.433	5.704	5.629	5.587	6.042	5.676	5.681	5.886	5.684	5.583
Al(IV)	2.503	2.567	2.296	2.371	2.413	1.958	2.324	2.319	2.114	2.316	2.417
Al(VI)	0.305	0.332	2.453	2.530	2.649	1.423	1.186	1.439	2.492	2.577	2.536
Ti	0.334	0.267	0.010	0.021	0.010	0.254	0.467	0.145	0.012	0.009	0.011
Fe*	3.210	3.267	5.298	5.230	5.105	2.808	2.686	2.874	3.512	3.451	3.462
Mn	0.030	0.029	0.054	0.067	0.069	0.048	0.044	0.045	0.066	0.065	0.068
Mg	2.035	2.201	4.091	4.040	4.031	3.696	3.967	4.329	5.606	5.745	5.846
Ca	0.022	0.000	0.002	0.000	0.000	0.008	0.191	0.006	0.009	0.007	0.000
Na	0.018	0.018	0.000	0.016	0.008	0.027	0.014	0.010	0.004	0.000	0.004
K	1.642	1.492	0.008	0.005	0.008	1.530	1.107	0.903	0.196	0.011	0.008

*Total Fe assumed to be in ferrous.

chloritization and vermiculitization are more complicate and will be discussed next in detail.

CHLORITIZATION

Analyses of the altered materials show that these are intermediate in chemical composition between biotite and chlorite end-member (Table 2). They are clearly consistent with notion that there is a apparently linear relationship between degree of structural reaction and the chemical composition. The linearity of the analyses indicates that the biotite composition is the main factor in determining chlorites composition in this reaction. However the deviation from the straight line between two end-members indicates that chlorite end-member composition changed with increased weathering on the assumption of biotite composition being constant. Because of the difference in the number of structural oxygens between biotite and chlorite, the ratios of each element were plotted in the diagrams indicating the weathering paths. The structural formulae in Table 2 indicate that the tetrahedral sheets of un-

Table 3. Electron microprobe analyses and structural formulae for biotites and altered products to vermiculites.

Element	R33									
	1	2	3	4	5	6	7	8	9	10
SiO_2	36.44	36.77	35.66	36.04	34.67	33.16	33.33	29.75	30.15	29.83
TiO_2	3.02	2.98	2.90	2.13	2.75	0.14	0.08	0.13	0.07	0.16
Al_2O_3	13.09	13.94	13.71	13.86	13.39	18.89	17.61	18.12	18.77	18.70
FeO*	18.90	18.68	20.17	19.74	20.91	20.88	18.60	22.78	23.65	23.87
MnO	0.16	0.13	0.17	0.13	0.08	0.16	0.13	0.18	0.20	0.18
MgO	11.80	9.53	10.01	9.91	8.97	8.89	9.82	10.74	9.91	9.20
CaO	0.00	0.61	0.51	0.81	0.89	0.86	0.69	0.52	0.57	0.69
Na_2O	0.11	0.20	0.54	0.27	0.11	0.13	0.24	0.12	0.14	0.07
K_2O	9.45	7.91	6.00	5.23	4.62	0.58	0.74	0.70	0.61	0.48
Total	92.97	90.75	89.67	88.12	86.39	83.04	81.30	83.04	84.07	83.18
	Number of ions on basis of 22 oxygens									
Si	5.717	5.841	5.737.	5.845	5.775	5.517	5.652	5.111	5.124	5.131
Al(IV)	2.283	2.159	2.263	2.155	2.225	2.483	2.348	2.889	2.876	2.869
Al(VI)	0.137	0.451	0.336	0.495	0.403	1.221	1.172	0.779	0.884	0.922
Ti	0.356	0.356	0.351	0.260	0.344	0.018	0.010	0.017	0.009	0.021
Fe*	2.480	2.482	2.714	2.677	2.913	2.905	2.638	3.273	3.361	3.434
Mn	0.021	0.017	0.023	0.018	0.011	0.023	0.019	0.026	0.029	0.026
Mg	2.760	2.257	2.401	2.396	2.227	1.833	2.154	1.905	1.717	1.598
	5.754	5.562	5.825	5.846	5.899	6.000	6.000	6.000	6.000	6.000
Mg**	0.000	0.000	0.000	0.000	0.000	0.372	0.329	0.846	0.794	0.761
Ca	0.000	0.104	0.088	0.141	0.159	0.153	0.125	0.096	0.104	0.127
Na	0.033	0.062	0.168	0.085	0.036	0.042	0.079	0.040	0.046	0.023
K	1.891	1.603	1.231	1.082	0.982	0.123	0.160	0.153	0.132	0.105
	1.925	1.768	1.488	1.308	1.176	0.696	0.693	1.135	1.076	1.017

* Total Fe assumed to be in ferrous.

** Mg contents treated as interlayer cations.

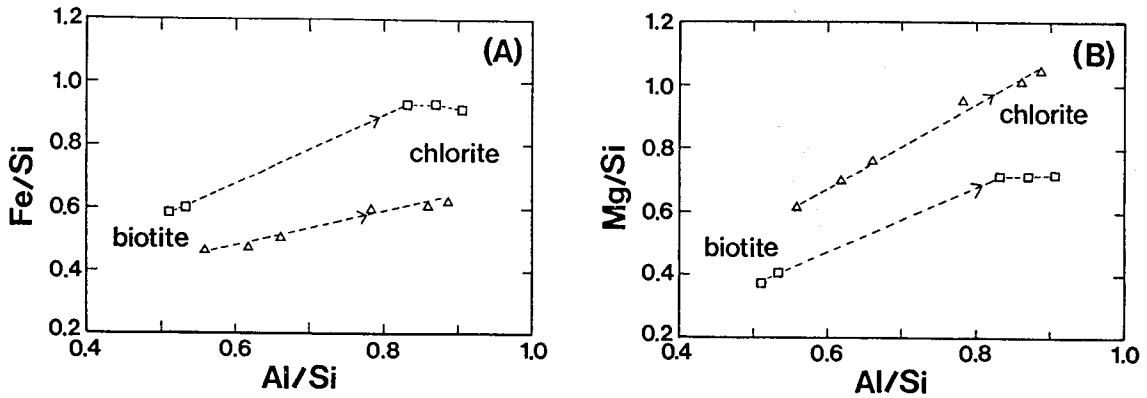

Fig. 2. Plots of Al/Si vs. Fe/Si (A) and Mg/Si (B) diagrams representing the alteration paths for biotite to chlorite (in atomic percentage). Open rectangular ; plots for R75 sample and open triangle ; plots for R76 sample.

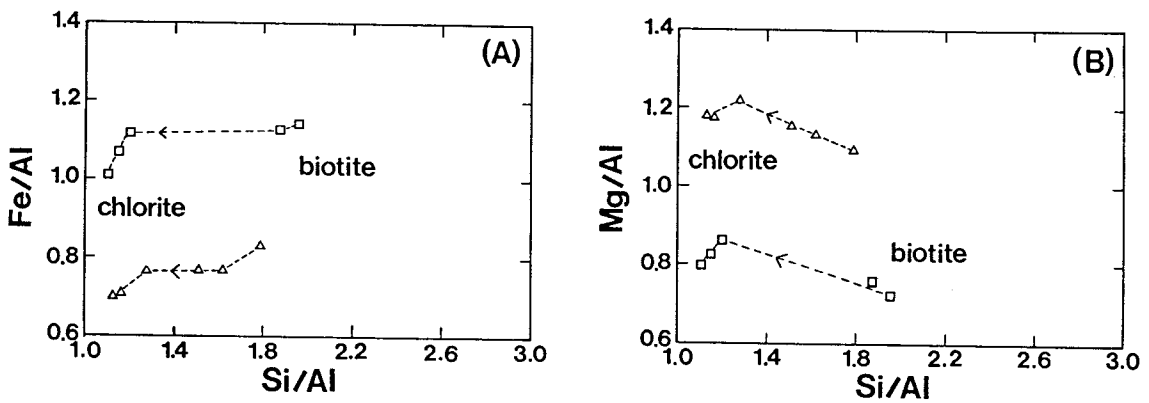

Fig. 3. Plots of Si/Al vs. Fe/Al (A) and Mg/Al (B) diagrams indicating the changes of variational trends in the late stage (in atomic percentage).Open rectangular ; plots for R75 sample and open triangle ; plots for R76 sample.

altered biotite and producted chlorite have a similar Si:Al ratio. The chemical results probably indicate that this chloritization is relatively Si-conservative reaction and the mica-like layer of the chlorite is inherited from the biotite.

Major differences between biotite and its chlorite reaction product are the high Al, Fe, and Mg contents of the chlorite-octahedral sheets, and the total loss of Ti from biotite. Thus although the tetrahedral sheets, appear to be inherited intact, there were free element exchange in the octahedral sheets. The contents of major elements in the unaltered biotite, intermediate, and chlorite phases were correlated in Fig.2 (by atomic percentage) for the relatively high Mg contents sample (R76) and the lower ones (R75), respectively. Weathering pahts of Al, Fe, and Mg relative to the Si contents show that these elements increase distinctly with increased weathering (Figs. 2-A and B). But the plots of the ratio Si/Al(T) (total Al) vs. Fe/Al(T) and Mg/Al(T) (Figs. 3-A and B) reveal the different trends, where the Fe/Al(T) and Mg/Al(T) ratios in the late stage are clearly decrease with increasing chloritization. It indicates that the rate of increase for Mg is higher than other two elements in the early stage, but in the late stage, the rate of increase for Al(T) is higher than the other ele-

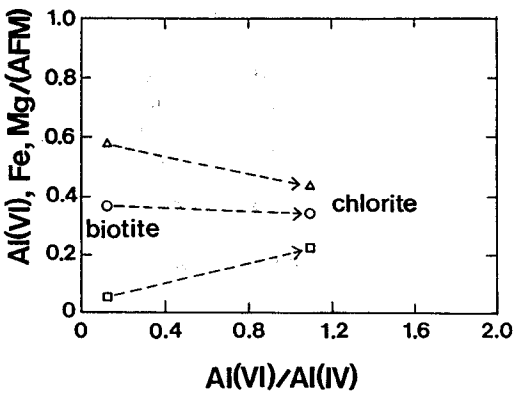

Fig. 4. Plots of Al(Ⅵ)/Al(Ⅳ) vs. Al(Ⅵ), Fe, and Mg/(Al(Ⅵ)+Fe+Mg) diagram indicating the substantial increase of Al(Ⅵ) in the late stage(in atomic percentage). Open rectangular;Al(Ⅵ)/(Al(Ⅵ)+Fe+Mg), open triangle ; Fe/(Al(Ⅵ)+Fe+Mg), and open circle ; Mg/(Al(Ⅵ)+Fe+Mg).

ments. That is, relative Al(VI) for the octahedral sheets increased especially in the late stage. Fig. 4 displays the relative changes of individual elements in the octahedral sheets for biotite-chlorite end-member pair (R75), obviously. The significant changes induced by these chemical variations are a dramatic increase of the Al-for-(Fe+Mg) octahedral substitution with increased weathering. This result is probably due to the factor of layer charge compensation. K-releasing from biotite causes the loss of total positive charge and then the two octahedral sheets produced by chloritization have to compensate the excess of negative charge. The increase of Al-for (Fe+Mg) octahedral substitution is considered as spontaneous change for the excess of negative charge to balance.

Two different mechanisms of chloritization were described by previous studies (Veblen and Ferry, 1983 ; Olives and Amouric, 1984 ; Yau et al.,1984 ; Eggleton and Banfield, 1985). Mechanism 1 is insertion of a brucite-like sheet into the interlayer region between the mica structures from which K^+ is removed, i.e., one biotite transforms one chlorite. This would entail a volume increase of about 40%. This mechanism would also require the introduction of a considerable number of Al, Fe, Mg, and H_2O, which are necessary for the construction of brucite-like layer. Mechanism 2 is the replacement of a mica-like structure by a brucite-like layer, i.e., a biotite layer has lost its silica tetrahedra and K^+ions and become a brucite-like layer. This mechanism results in a volume loss of about 30%. Table 4 shows the cation budgets for both mechanisms for the selected sample (R75) calculated on the assumption Si presumed to be in the form of H_4SiO_4 as in Ferry (1979) and Veblen and Ferry (1983). Mechanism 1 proceeds at nearly constant Si, releasing K, Ti, and H^+ and requring a large number of Al, Fe, and Mg to the octahedral sheets besides water. On the other hand, mechanism 2 produces much differnt results. The overriding chemical consequences of this reaction are the removal of Si and K and the addition of H^+, with relatively minor removal of Al, Fe, and Mg.

Table 4. Cation budgets for biotite to chlorite replacement(R75).

Cation	1 Biotite → 1Chlorite (Mechanism 1)			
	Biotite	+	→ Chlorite	+
Si	5.50	—	5.59	—
Al	2.81	2.25	5.06	—
Ti	0.33	—	0.01	0.32
Fe	3.21	1.90	5.11	—
Mg	2.04	1.99	4.03	—
Ca	0.02	—	0.00	0.02
K	1.64	—	0.01	1.63
H_4SiO_4	-	0.09	—	—
H_2O	-	11.64	—	—
H^+	4.00	—	16.00	11.64
Cation	2 Biotite → 1Chlorite (Mechanism 2)			
	Biotite	+	→ Chlorite	+
Si	11.00	—	5.59	-
Al	5.62	—	5.06	0.56
Ti	0.66	—	0.01	0.65
Fe	6.42	—	5.11	1.31
Mg	4.08	—	4.03	0.05
Ca	0.04	—	0.00	0.04
K	3.28	—	0.01	3.27
H_4SiO_4	—	—	—	5.41
H_2O	—	9.04	—	—
H^+	8.00	10.36	16.00	—

Another chemical aspect of these reactions involves the role of H^+ ion. The two reaction mechanisms require very different behavior of H^+. As shown in Table 4, mechanism 1 should produce a large number of H^+ ions, while

mechanism 2 would require an influx of H^+. T hus mechanism 2 would be favored in an acidic environment relative to mechanism 1. Considering the earth-surface environment, a source for the H^+ required for mechanism 2 presumably existed during the alteration. On the microscopic examination, some sphene and epidote were observed in altered regions as texturally secondary minerals. Mechanism 2 releases some cations required in the crystallization of these alteration products. And this mechanism would supply the Al contents, which are necessary for the Al-for-(Fe+Mg) octahedral substitution occurring in the chloritization discussed above, from the dissolved one mica- like layer.

Considering the aspects of the chemical and petrographic factors, the chloritization studied here indicates that mechanism 2 is possibly dominant processes. The biotite-chlorite reaction provides a good example of structural inheritance in an alteration process. The biotite 2:1 layer is passed completely to the chlorite occurring the octahedral cation re-equilibriation, predominantly Al-for-(Fe+Mg) octahedral substitution. The tetrahedral sheet is transferred intact.

VERMICULITIZATION

Analyses of the biotite and of their weathering pruducts are listed in Table 3 and strutural formulae are calculated on the basis of 22 oxygens and total Fe contents were assumed to be in ferrous state and the octahedral sites of altered products to be in complete occupancy. Then the Mg contents equal to the excess of octahedral cations were subtracted from octahedral sites and treated as interlayer cations (Table 3). These data show the common variational trends of K-leach-

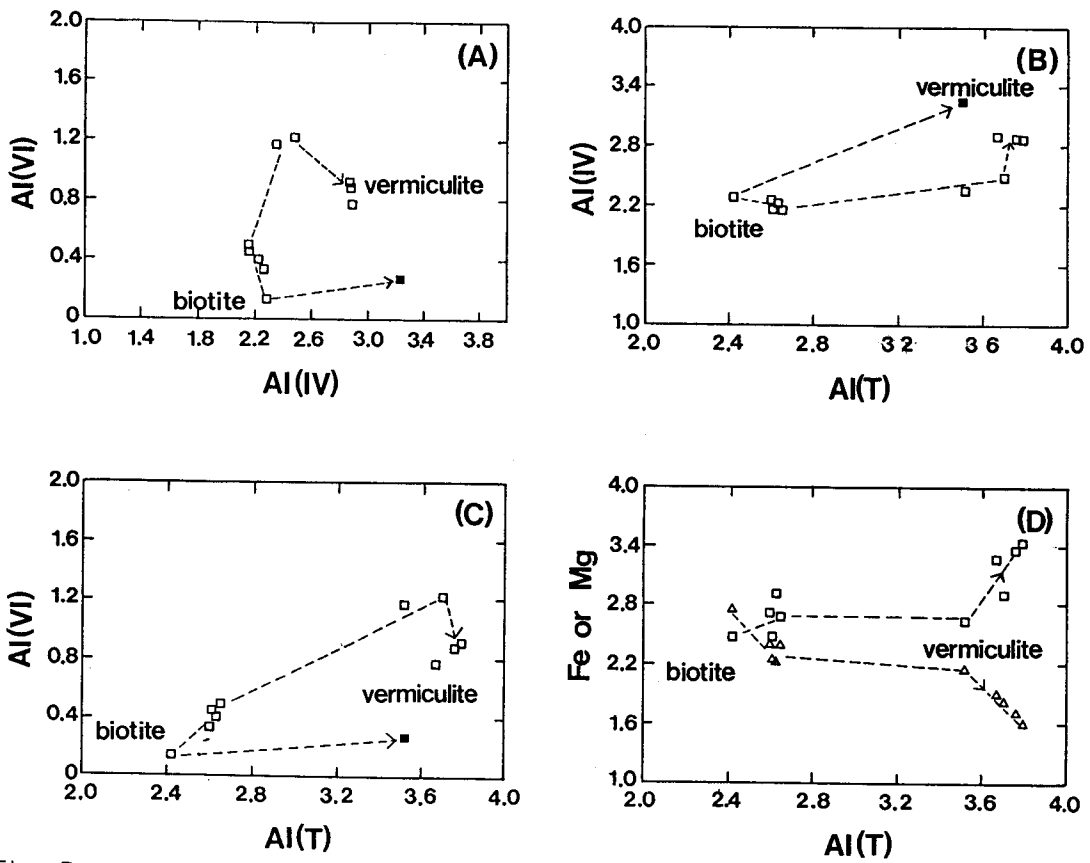

Fig. 5. Variational curves for biotite to vermiculite (in atomic percentage). (A) ; Plots of Al (Ⅳ) vs. Al (VI), (B) ; Al(T) vs. Al(Ⅳ), (C) ; Al(T) vs. Al(VI), and (D) ; Al(T) vs. Fe (open rectangular) and Mg (open triangle). Solid rectangular indicates the vermiculite composition treated the total Fe as ferric.

ing and Ca-enriching with increasing vermiculitization. And total Mg contents were relatively conservative during the vermiculitization. But the substitutions of the mica-like layer are more complicate. Relations of Si, Al, Fe, and Mg were shown in Figs. 5-A, B, C, and D. There are significant deviation from the straight line between two end-member compositions. It indicates that producted vermiculite composition changed with increased weathering on the assumption of biotite composition being constant. The weathering of biotite appears to have taken place in two stages. In the early stage of vermiculitization, in which biotite alters into interstratified phases, weathering paths of the Al, Fe, and Mg contents show distinctly linearity, where Al (T) and Al (VI) increase, Al (IV) decrease and Fe and Mg remain nearly constant or decrease slightly with increasing vermiculitization. The chief changes inferred by these relations are a continuous decrese of the Al-for-Si tetrahedral substitution together with a general increase of the Al-for-(Fe+Mg) octahedral substitution with increased weathering. These substitutions are considered as spontaneous reactions for the excess of negative charge to balance as weathering increase and are in good agreement with currently accepted weathing trends (Proust et al.,1986 ; Fordham, 1990a, 1990b). However, in the late stage that interstratified phases alter into vermiculite, the different trends are observed, where the Mg contents in octahedral sheet decrease and the Al(T) contents increase constantly, whereas the Al(Ⅳ) and Fe contents increase substantially and the Al(VI) contents are decreasing slightly. Granting that total Fe are assumed to be in ferric state in the vermiculite phase, the Fe contents also increase significantly. These chemical changes indicates that the Al-for-Si substitution in tetrahedral sheets increases clearly together with the remains and/or a slight decrease of the Al-for-(Fe+Mg) octahedral substitution in spite of the increase of Al(T) with increased weathering.

Two controlling factors can be inferred concerning the change of the late stage ; (1) the increase of a number of Fe and Al in structural units and (2) the oxidation of ferrous Fe in octahedral sheets (Moon et al ., 1992). The increase of the Fe and Mg contents and the oxidation of ferrous Fe contents affect significantly the increase of positive charge and can bring out the surplus of positive charges in the mica-like layer. If total Fe contents are assumed to be in ferric, degrce of the Al-for-Si substitution will be much higher than that in ferrous. This tetrahedral substitution can be also considered as the charge compensation effect for the surplus of positive charge by the oxidation and the enrichment of Fe in octahedral sites. The Al substitution for octahedral sites is interfered by the increase of the Al substitution for tetrahedral sites in spite of the increase of Al(T).If total Fe are calculated as ferric,degree of this substitution will be much less than that as ferrous. The two types of reaction mechanisms for the transformation of biotite to vermiculite similar to those of chloritization were proposed by Banfield and Eggleton(1988). The most commonly observed reaction by them is mechanism 1 which involves loss of interlayer K and introduction of a hydrated cation-interlayer, expanding the layer thickness. Mechanism 2 involves

Table 5. Cation budgets for biotite to vermiculite replacement (R33).

Cation	1 Biotite →		1 Vermiculite(Mechanism 1)	
	Biotite	+	→Vermiculite	+
Si	5.72	—	5.13	—
Al	2.42	1.37	3.79	—
Ti	0.36	—	0.02	0.34
Fe	2.48	0.95	3.43	—
Mg	2.76	—	2.36	—
Ca	0.00	0.13	0.13	—
K	1.89	—	0.11	1.63
H_4SiO_4	—	—	—	0.59
H_2O	—	n*+2.36	n*	—
H^+	4.00	2.36	4.00	—
Cation	2 Biotite →		1 Vermiculite (Mechanism 2)	
	Biotite	+	→Vermiculite	+
Si	11.44	—	5.13	—
Al	4.84	—	3.79	1.05
Ti	0.72	—	0.02	0.70
Fe	4.96	—	3.43	1.53
Mg	5.52	—	2.36	3.16
Ca	0.00	0.13	0.13	—
K	3.78	—	0.11	3.67
H_4SiO_4	—	—	—	6.31
H_2O	—	n*+1.24	n*	—
H^+	8.00	18.76	4.00	—

* n indicates the number of H_2O in interlayer region of vermiculite.

the conversion of two biotite to one vermiculite layer, with consequent release of most of the elements of one layer and a volume decrease. Table 5 shows the cation gain-and-loss for both mechanisms for the selected biotite (R33) calculated on the same assumptions as those in chloritization. Mechanism 1 proceeds releasing K, Si, and Ti and requiring Al, Fe, water, H^+, and a small number of Ca, whereas mechanism 2 requires only water, H^+, and a small number of Ca and releases a large amount of cations. The additional cations required by mechanism 1 would be supplied plentifully by mechanism 2 by complete dissolution of one biotite layer, which maybe less commonly occurred. Then the addition of the Fe contents in the vermiculitization described above would be explained by this reaction.

The different aspect of these reactions relative to chloritization involves the role of H^+ ion, where the vermiculitization should require a large number of H^+ ions for both mechanisms. Therefore the vermiculitization would be favored in an acidic environment. Considering that any other altered minerals are not observed on the microscopic examination, then maybe the mechanism 1 would be considered as the dominant alteration mechanism and the mechanism 2 would also occur less commonly as the result of TEM observation by Banfield and Eggleton(1988).

Status of Fe in the vermiculitization is a main factor controlling the substitutions in the mica-like layer. And the Mg contents in the octahedral sites and interlayer sites can not be determined separately by microprobe analysis. Then the structural formulae of vermiculite were recalculated on basis of serveral assumptions as the same in Moon et al.(1992) as following (Table 6) ; (1) total Fe contents are assumed to be in ferrous state and the Mg contents equal to the excess of cations in octahedral sites are treated as interlayer cations, (2) total Fe contents are assumed to be in ferric state and if the sum of octahedral cations exceeds 6, the Mg contents equal to the excess of cations are treated as interlayer cations, and (3) total Fe contents are assumed to be in ferric, and a part of the Mg content are treated as interlayer cations until reaching the layer charge to 1. 2.

In the case of (1), the vermiculite shows relatively high layer charge and the sum of exchangeable cations. In fact, this value would be much higher, supposing some vacancies in octahedral sites. In the case of (2), the vermiculite produces adequate vacant site. But the layer charge and the the sum of exchangeable cations are much less than those of general vermiculite composition. In the case of (3), the vermiculite shows the reasonable structural formular, layer charge, and the sum of exchangeable cations. However, the octahedral sites reveal the excessive vacancies. And then the recalculation is performed on the basis of the another assumption that the sum of exchangeable cations is 130 meq. /100g and the octahedral vacant sites are 0.4 on the basis of 22 oxygens. Therefore a part of the Mg contents are treated as interlayer cations until reaching the sum of exchangeable cations to 130 meq./100g and a part of the Fe contents are as-

Table 6. Calculated structural formulae and exchangeable cation values for representative vermiculite (R33) on the basis of several assumptions discussed in text.

Sample Name	(1)	(2)	(3)	(4)
Si	5.131	4.760	4.760	4.886
Al(IV)	2.869	3.240	3.240	3.114
Al(VI)	0.922	0.276	0.276	0.496
Ti	0.021	0.019	0.019	0.020
Fe^{3+}	0.000	3.185	3.185	2.099
Fe^{2+}	3.434	0.000	0.000	1.171
Mn	0.026	0.024	0.024	0.025
Mg	1.598	2.188	1.765	1.789
	6.000	5.693	5.270	5.600
Mg*	0.762	0.000	0.423	0.457
Ca	0.127	0.118	0.118	0.121
Na	0.023	0.022	0.022	0.022
K	0.105	0.098	0.098	0.100
	1.017	0.237	0.661	0.701
L.C.	1.91	0.36	1.20	1.28
Calculated exchangeable cations (meg./100g)				
EXC(Mg)	147.37	0.00	88.32	92.94
EXC(Ca)	24.61	24.61	24.61	24.61
EXC(Na)	2.26	2.26	2.26	2.26
EXC(K)	10.19	10.19	10.19	10.19
Sum	184.43	37.06	125.38	130.00

*Mg contents treated as interlayer cations.

sumed to be in ferric until reaching the octahedral vacant sites to 0.4. The result is shown as the column (4) in Table 6. In this case, the vermiculite shows more reasonable structural formular, layer charge (1.28), and relatively high ferric Fe contents. This result indicates that the vermiculitization requires the oxidation of at least a part of ferrous Fe contents and a significant number of Mg are cosidered as interlayer cations. The relative timing of the oxidation of Fe is not clear. Oxidation of Fe, however, did probably not occur in the reaction-initiating stage but in the late stage. This is supported by the increase of the Al-for-Si tetrahedral substitution in the late stage. Oxidation was apparently compensated by the re-distribution of some octahedral Al replacing Si in the tetrahedral sheets.

SUMMARY AND CONCLUSIONS

Biotite weathering, as observed here, can be subdivided into the chloritization and vermiculitization. The chloritization is characterized by Si-conservative reaction and relatively dramatic increase of the Al-for-(Fe+Mg) octahedral substitution with increased weathering probably in order to compensate the excess of negative charge in the mica-like layer. The vermiculitization is distinctly characterizad by total Mg-conservative and Ca-enriching exchange reactions. The vermiculitization in the early stage proceeded by means of a continuous decrease of the Al-for-Si tetrahedral substitution and a increase of the Al-for-(Fe+Mg) octahedral substitution, which agrees well with the general argument of the increasing dioctahedral character of the clay minerals as weathering increases. It differs, however, distinctly in the late stage, that is, Al(Ⅳ) and Fe increase substantially. It can be considered as the enrichment and oxidation of Fe. These two alterations can be performed by both the 1:1 and 2:1 reaction mechanisms. Considering the aspects of the chemical changes, microscopic observations, and environmental factors, mechanism 2 is probably dominant process for the chloritization, whereas mechanism 1 for the vermiculitization. The Al contents demended by the Al-for-(Fe+Mg) substitution in the chloritization would be supplied by reaction mechanism 2. And the Fe contents that are necessary for the chemical change in the late stage in the vemiculitization would be also supplied from a completely dissolved biotite by less common mechanism. 2. Recalculations of the structural formular for vermiculite on the basis of several assumptions indicate that the oxidation of Fe is necessary for the vermiculite to form the reasonable structural formular. The relative timing of the oxidation of Fe probably would be in the late stage of vermiculitization, which is supported by the increase of the Al-for-Si tetrahedral substitution in the late stage.

ACKNOWLEDGEMENTS

This work has been carried out with support from Yonsei University to HSM. We also ackcnowledge a partial support from the Center for Mineral Resources Research sponsored by the KOSEF.

REFERENCES

Banfield, J. F. and Egglenton, R. A. (1988) Transmission electron microscope study of biotite weathering. Clays and Clay Min. , v. 36, p. 47-60.

Bence, A. E. and Albee, A. L. (1968) Empirical correction factors for the electron microanalysis of silicates and oxides. J. Geol., v. 76, p.382-403.

Eggleton, R. E. and Banfield, J. F. (1985) The alteration of granitic biotite to chlorite. Am. Min., v.70, p.902-910.

Ferry, J. M. (1979) Reaction mechanisms, physical conditions, and mass transfer during hydrothermal alteration of mica and feldspar in granitic rocks from south-central Maine, U.S.A. Contr. Min. Petrol., v.68, p.125-139.

Fordham, A.W.(1990a) Treatment of microanalyses of intimately mixed products of mica weathering. Clays and Clay Min., v.38, p.179-186.

Fordham, A.W.(1990b) Formation of trioctahedral illite from biotite in a soil profile over granite gneiss. Clays and Clay Min., v. 38, p.187-195.

Iijima, S. and Zhu, J.(1982) Electron microscopy of a muscovite-biotite interface. Am Min., v.67, p.1195-1205.

Moon, H.-S., Song, Y. and Lee, S.Y.(1992) Supergene vermiculitization of phlogopite and biotite in ultramafic and mafic rock (in submitted).

Olive, J. and Amouric, M.(1984) Biotite chloritization by interlayer brucitization as seen by HRTEM. Am. Min., v. 69, p.869-871.

Proust, D, Eymery, J.P. and Beaufort, D.(1986) Supergene vermiculitization of a magnesian chlorite. Iron and magnesium removal processes. Clays and Clay Min., v.34, p. 572-580.

Spear, F.S. and Kimball, K.L.(1984) Recamp-A fortran Ⅳ program for estimating Fe^{3+} contents in amphiboles. Computers & Geoscience, v.10, p.317-325.

Veblen, R.D.(1983) Microstructures and mixed layering in intergrown wonesite, chlorite, talc, biotite, and kaolinite. Am.Min., v.68, p.566-580.

Veblen, R.D. and Ferry, J.M.(1983) A TEM study of the biotite-chlorite reaction and comparision with petrologic

observation. Am. Min., v.68, p.1160-1168.
Yau, Y.-C., Anovitz, L.M., Essene, E.J., and Peacor, D.R. (1984) Phlogopite-chlorite reaction mechanisms and physical conditions during retrograde reactons in the marble formation, Franklin, Neu Jersey.Contr. Min.Petrol.,v. 88, p.299-306.

Manuscript received 2 July 1991

청양지역 각섬석 편마암의 녹니석화 및 질석화 작용 연구

송윤구 · 문희수

요약: 청양지역의 각섬석편마암을 구성하는 흑운모는 심한 변질작용을 받아 녹니석화 및 질석화되어있다. 흑운모와 변질작용의 산물들에 대한 체계적인 전자현미분석은 이들 변질작용의 진행과정에서의 화학적 변화양상에 대한 중요한 정보를 제공해 준다. K와 Ti의 이탈작용은 두 변질작용에서 모두 나타나는 공통된 현상이지만, 흑운모의 사면체화 팔면체에서의 치환양상은 두 작용에서 전혀 다르게 나타난다. 그러나, 두 작용은 모두 층간의 전기적 균형을 이루려는 치환양상을 보이고 있다. 녹니석화 작용에서는 사면체내의 Si수가 일정하게 유지되며, 팔면체내에서의 Fe 및 Mg에 대한 Al의 치환양상이 두드러지게 나타난다. 이와는 달리, 질석화작용의 경우, 초기에는 일반적인 변질작용의 경향과 일치하는 dioctahedral화 되는 치환작용, 즉, Al의 팔면체에 대한 치환도가 증가하는 경향을 보이지만, 후기에서는 Al의 사면체로의 치환과 Fe의 팔면체 치환이 두드러지게 나타나는데, 이는 Fe의 양의 증가와 산화작용에 의한 결과로 생각된다. 두 변질작용은 모두 하나의 흑운모 구조가 곧바로 하나의 녹니석 및 질석으로 변화하는 과정과 두개의 흑운모 구조가 하나의 녹니석 및 질석으로 변화하는 과정이 제시되어 있는데, 현미경관찰 결과 및 화학적인 변화양상 등을 고려하여 볼 때, 녹니석화작용의 경우는 후자의 변화과정이 우세하였을 가능성이 높으며, 이 작용에 의해 변질과정이 요구되는 Al의 자체공급도 가능할 수 있다. 반면에 질석화 작용은 전자의 변화과정이 우세하였을 것으로 보이는데, 후기의 치환작용에서 요구되는 Fe의 증가는 보다 드물게 병행된 두개의 흑운모층이 하나의 질석으로 되는 작용의 결과로 생각할 수 있다. 질석화작용은 Fe의 전하상태가 매우 중요한 역할을 하는 것으로 보이는데, 이에 대한 해석을 위하여 몇가지 가정하에서 구조식을 재계산하여 보았다. 그 결과 질석에 적절한 구조식이 되기 위해서는 상당량의 Fe의 산화를 요구하게 되는 것으로 나타났다. 산화작용의 시기는 확실하지는 않지만, 치환작용변화가 일어난 질석화작용의 후기일 가능성이 높다.